Assessing additional fuel consumption from cabin thermal comfort and auxiliary needs on the worldwide harmonized light vehicles test cycle

Charbel Mansour[1], Wissam Bou Nader[2], Florent Breque[3], Marc Haddad[1], Maroun Nemer[3]

[1] Lebanese American University, Industrial and Mechanical Engineering Department, New York, United States
[2] PSA Group, Centre technique de Vélizy, Vélizy, France
[3] Ecole des Mines de Paris, Center for Energy Efficiency of Systems, Palaiseau, France

Abstract:
Standards for fuel consumption and carbon dioxide emissions are implemented worldwide in most light-duty vehicle markets. Regulatory drive cycles, defined as specific time-speed patterns, are used to measure levels of fuel consumption and emissions. These measurements should realistically reflect real world driving performance, however there is increasing concern about their adequacy due to the discrepancies observed between certified and real world consumption and emissions values. One of the main reasons for the discrepancy is that current testing protocols do not account for non-mechanical vehicle energy needs, such as passengers' thermal comfort needs and the use of electric auxiliaries on-board. Cabin heating and cooling can especially lead to considerable increase in vehicle energy consumption. This paper presents a simulation-based assessment framework to account for the additional fuel consumption related to the cabin thermal energy and auxiliary needs under the worldwide-harmonized light vehicles test procedure (WLTP). A vehicle cabin model is developed and the thermal comfort energy needs are derived for cooling and heating, depending on ambient external temperature under cold, moderate and warm climates. A modification to the WLTP is proposed by including the generated power profiles for thermal comfort and auxiliary needs. Dynamic programming is used to compute the fuel consumption on the modified WLTP for a rechargeable series hybrid electric vehicle (SHEV) architecture. Results show consumption increases of 20% to 96% compared to the currently adopted WLTP, depending on the considered climate.

Keywords:
WLTP, thermal comfort, cabin model, dynamic programming, heating and cooling, auxiliary.

1. Introduction

There has been ever growing interest over the past few years for improved estimation procedures of vehicle fuel consumption and emissions, especially in light of recent controversy regarding the under-estimating of performance between original equipment manufacturers (OEM) tests and real world driving conditions. This has pushed the United Nations Economic Commission for Europe (UNECE) to define a new Worldwide harmonized Light vehicles Test Procedure (WLTP) as a new global standard for assessing fuel consumption and emissions, starting in September 2017 [1]. The WLTP consists of a number of procedures for testing a vehicle on driving cycles, known as WLTC (Worldwide harmonized Light vehicles Test Cycles) which are designed to be more representative of real world driving behaviors compared to the outdated NEDC (1997). This is done by incorporating low, medium, high and extra-high loads on the vehicle [2] which will reflect

higher average real world fuel consumption and emissions from vehicle propulsion needs [3-6].

However, the WLTP still doesn't consider non-mechanical vehicle energy needs which impact fuel consumption and emissions, such as those for ensuring passenger thermal comfort by cabin heating and cooling, as well as the need to power auxiliary systems. It is well established that thermal comfort and electric needs account for a substantial share of overall vehicle energy needs, which can have a significant impact on the electric autonomy of hybrid and electric powertrains, especially under extreme climate conditions. In fact, thermal comfort needs vary considerably depending on factors such as cabin internal temperature, external temperature, type of vehicle, trip length, among several others [7, 8]. Therefore, in order to bring regulatory drive cycle test results closer to real world consumption, thermal comfort and electric needs in real world conditions should be accounted for. So far, only an optional U.S. test for assessing energy consumption and emissions, the SC03 Supplemental Federal Test Procedure (SFTP) [9], addresses some of these non-mechanical energy needs by considering the air conditioning only. Farrington et al. [10] shows that 3,500W peak A/C load reduces the driving range of a sedan EV by 36% on the SC03, while it increases the consumption of an HEV by 57%.

Several studies have demonstrated the impacts of cabin heating on energy consumption. For example, EV energy consumption has been shown to increase by up to 32% with the decrease in ambient temperature, and a reduction in electric driving range of up to 24% has been measured when a heating system is operated [11].

Other studies have addressed the impacts of cabin cooling on energy consumption, where in hot climates vehicle air conditioning (A/C) loads can become significant enough to even outweigh rolling resistance loads [12]. It has also been established that cooling energy consumption in plug-in hybrid electric vehicles (PHEV) is strongly dependent on climate, varying considerably among different regions of the US [13]. The energy required for cabin cooling has been shown to reduce the range of PHEV between 35% to 50% depending on outside weather conditions [9]. [10] shows that a 1,000W steady-state A/C load in a small sedan EV reduces the SC03 range by 16%, and increases the fuel consumption by 16% in an HEV. For EVs, the A/C is used also to heat up the vehicle, which in winter can reduce electric autonomy by 8%-24% depending on the external temperature [14].

Some studies assessed the impacts of both cabin heating and cooling on vehicle energy consumption. [11] estimated an 850W cooling, 1,200W cooling and 2,200W heating of thermal power needs when outside temperatures are respectively 25°C, 35°C and -5°C. Results show an EV range reduction on NEDC between 3% and 9% under the cooling scenarios and 22% under the heating scenario when compared to the baseline scenario of 700W auxiliary load consumption. Similarly, Zhang et al. [15] presents the simulation results of an EV performance on NEDC with cooling and heating needs. Results show 17.2% to 37.1% range reduction due to cooling load in summer, and a 17.1% to 54% range reduction when using a PTC heater in winter. Testing of a Ford Focus EV on the Urban Dynamometer Driving Schedule (UDDS) drive cycle showed a reduction in range of 53.7% due to air conditioning and 59.3% due to heating [16]. Cooling and heating have also been shown to reduce the UDDS driving range of a Nissan Leaf by 18% and 48%, respectively [17].

Few studies have considered the impact of auxiliaries on vehicle energy consumption. [10] shows that an increase in the accessory load from 500W to 3,500W will cause the EV range on repeated FUDS cycle to decrease by 38%, and by 36% on SC03 cycle.

Across all the assessments surveyed above, there was no common framework for assessing the impacts of thermal comfort and electric needs on vehicle energy consumption, such as a drive cycle which incorporates cabin heating, cooling and auxiliary needs in a way to reflect real world driving conditions.

On the industry side, OEMs work continuously to reduce the amount of energy used for cabin environment control through a variety of techniques, such as advanced window glazing, individual cooling control, heated/cooled seats, parked car ventilation [18], recirculation strategies and air cleaning [10]. But despite these advances, OEMs continue to face significant challenges in meeting cabin energy consumption needs, especially with electric vehicles (EVs) where cabin thermal comfort has to be ensured from relatively inefficient technologies which reduce electric autonomy, such as electric heaters. In this respect, manufacturers might be well served to accurately assess the real world consumption of their electrified vehicles in order to better fulfill cabin thermal energy needs with the appropriate technologies. For example, depending on cabin heating needs in different climates, the choice of heating technologies might be different and the design of the vehicle architecture might be optimized to deliver those particular needs.

Hence, in order to better inform future assessments of fuel consumption in real world conditions, this study proposes a modification to the WLTP that includes cabin thermal comfort and electric auxiliary needs in addition to vehicle propulsion needs. The resulting amended WLTP will be denoted in the rest of the study as “modified WLTP”. The study starts with a framework for redefining the vehicle energy needs, as presented in section 2. This includes a methodology for defining the heating and cooling power profiles under different climates. To that end, a vehicle cabin thermal model is developed and presented in the same section. The resulting heating and cooling power profiles, in addition to the auxiliary power needs are used to propose a modified WLTP that is more representative of real world conditions under three climate categories (hot, moderate and cold). Section 3 presents the modelling of the powertrain for a rechargeable SHEV, which uses dynamic programming in order to assess the additional fuel consumption from heating, cooling and electrical power needs under the three climate categories. The corresponding results are discussed in section 4, and compared to the consumption results of a baseline scenario where only mechanical traction needs are considered.

2. Framework for accounting of vehicle thermal cabin and auxiliary power needs on the WLTP

This section presents the framework for developing a modified WLTP that takes into account the vehicle thermal and electrical energy needs that are not currently considered. The framework consists of a two-step method for generating vehicle thermal and electrical power profiles. These power profiles would be used in combination with the WLTC velocity profile for a more representative fuel and emissions assessment. The framework is summarized in Figure 1.

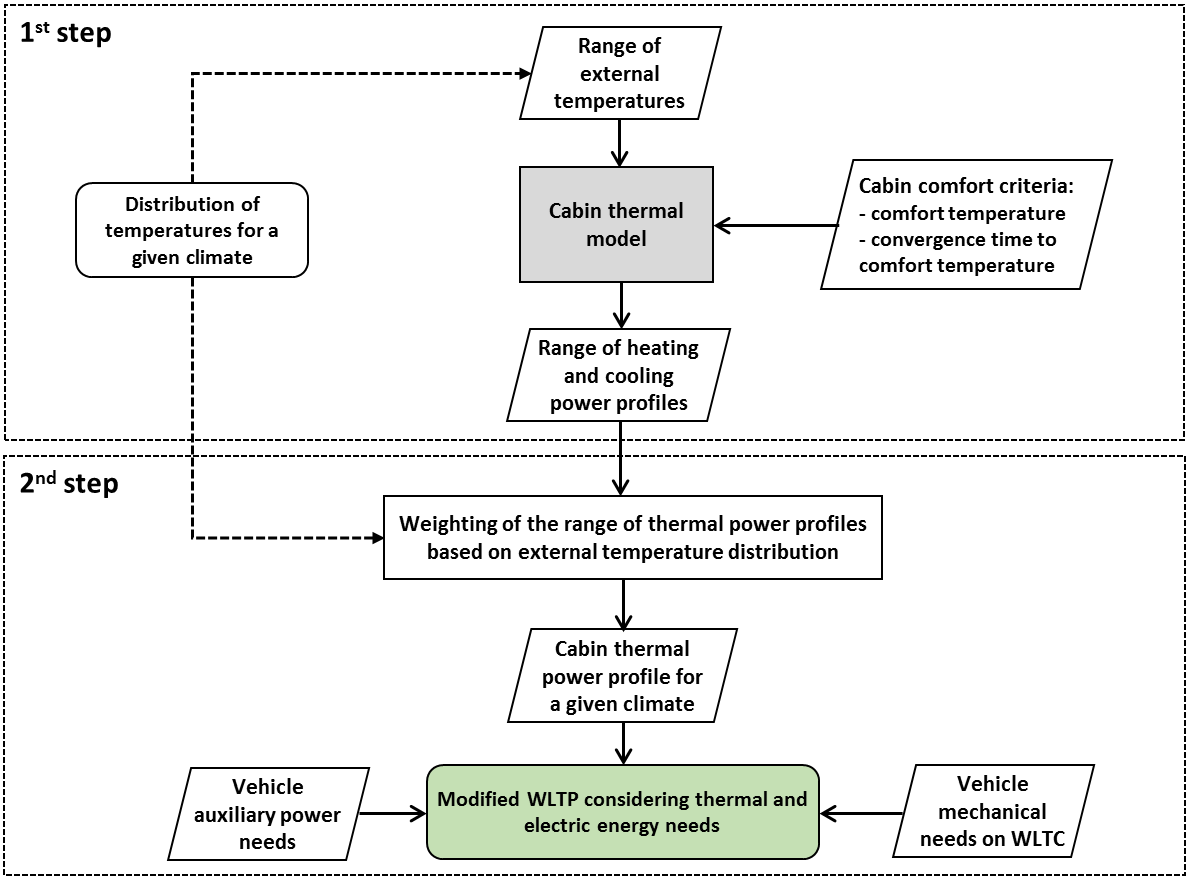

Figure (1): Framework for redefinition of WLTP considering thermal and electrical energy needs.

The first step consists of feeding the cabin thermal model with the range of external temperatures for a given climate, as well as the cabin comfort criteria consisting of the internal comfort temperature and the corresponding convergence time to this temperature. The outcome is a range of power profiles emulating the cabin thermal energy needs corresponding to the different external temperatures.

In the second step, the different power profiles are weighted according to the frequency of occurrence of external temperatures for a given climate over time. This generates a representative power profile for given climate conditions. In addition, a vehicle electric profile for powering auxiliaries is derived.

When these two generated power profiles are combined with the current WLTC drive cycle, the final outcome becomes the modified WLTP considering thermal and electrical needs.

The rest of this section goes into the details of each component of the framework described above. The vehicle cabin model is presented in section 2.1, and the range of thermal energy profiles are calculated in section 2.2. The weighting of thermal power profiles based on temperature distribution, in addition to the determination of electric consumption based on a survey of industry best practice, are presented in section 2.3. Finally, the modified WLTP is proposed in that same section based on the combination of the existing WLTC cycle and the developed power profiles.

2.1 Thermal Vehicle Model

The first step in the proposed framework is to predict the thermal energy needs. Hence, a cabin thermal model is developed by the authors for that purpose using the Dymola-Modelica software. The model consists of several sub-models as shown in Figure 2, and is described in detail in [19]. The relevant workings of the model are summarized in this section.

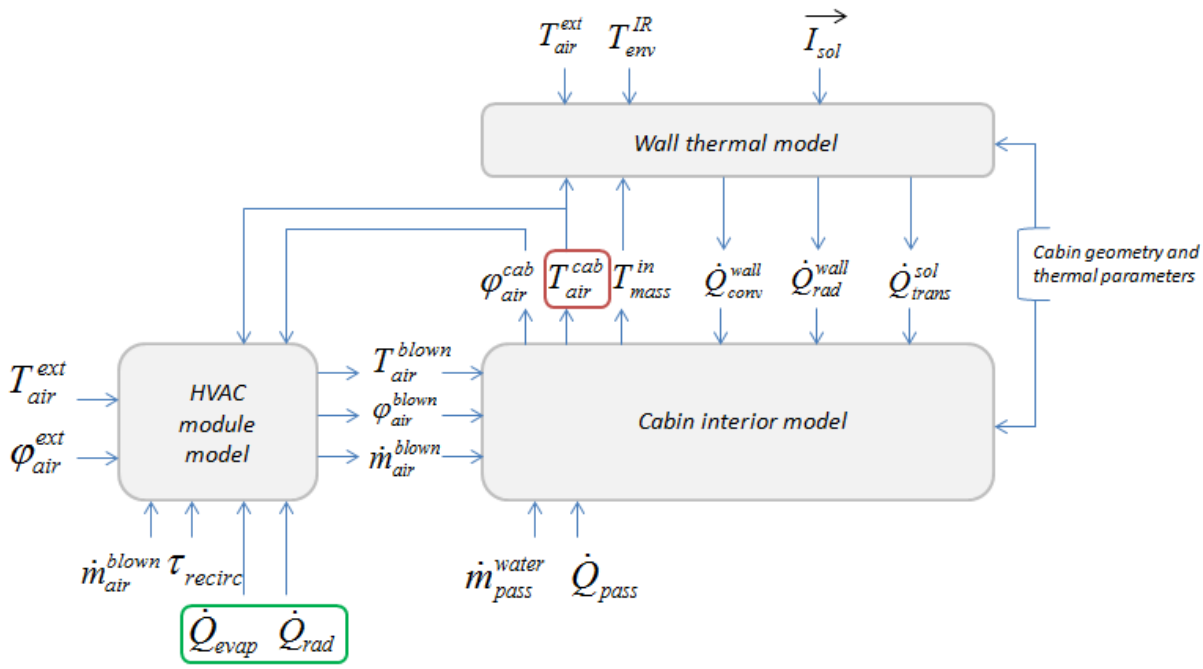

Figure (2): Schematic of the cabin thermal model.

The cabin interior model represents how the cabin interior is cooled and heated by the HVAC system and the external environment through the cabin walls.

The monozonal modelling approach is considered, where the cabin air volume is represented by a single thermal node at a uniform temperature T_{air}^{cab}. Energy exchanges happen between the cabin air and cabin materials such as the seats and dashboard, as well as by the passengers thermal flow $\dot{Q}_{pass}$. All physical elements in the cabin are at T_{mass}^{int} accounting for all internal solid mass.

Exchange with the external environment happens through the cabin walls represented the wall thermal model. Knowing the temperatures of the two internal nodes above, and given the outside conditions (the external air temperature T_{air}^{ext}, the infra red environment temperature T_{env}^{IR} and the solar vector $\overrightarrow{I_{sol}}$), the wall model determines the convective heat flow $\dot{Q}_{conv}^{wall}$, the radiative heat flow $\dot{Q}_{rad}^{wall}$ and the transmitted solar heat flow into the cabin through glazing $\dot{Q}_{trans}^{sol}$ absorbed by the internal mass. The dynamic thermal balances at the wall external and internal surfaces are applied, taking into account the wall thermal capacitances. As for the internal thermal paths, the external convection and radiation conductance are taken into account. The absorbed solar flux on the opaque surfaces is also considered.

The HVAC sub-model represents how the HVAC system works in exchanging energy with the cabin interior and the outside environment. The HVAC model first determines the properties of the mixing air between the fresh air at T_{air}^{ext} and the recirculation air at T_{air}^{cab} given the blown air mass flow rate $\dot{m}_{air}^{blown}$ (which includes a steady or cabin comfort state and a transient or convergence to cabin comfort state) and the recirculation ratio τ_{recir}. Then, the evaporator cooling capacity $\dot{Q}_{evap}$ and/or the radiator heating capacity $\dot{Q}_{rad}$ are injected into the air flow to compute the blown air temperature T_{air}^{blown}. Finally, taking into account the thermal loads from the blown air, from the walls and also from the passengers, the cabin interior model solves the dynamic energy balances at the cabin air node and at the internal mass node.

In addition to the thermal computations, the model accounts for changes in the relative humidities φ at different locations.

The model calculates both the transitory and steady-state thermal needs in the cabin: first, given a thermal power need, the model computes the dynamic response (i.e. transitory state) of the cabin air temperature T_{air}^{cab}, producing the transitory curve from the initial temperature; and, given a target in terms of steady-state thermal comfort, the model determines the thermal power needs, i.e. the evaporator cooling capacity and the radiator heating capacity.

The model requires a full list of parameters. For conciseness, only the most relevant parameters needed for the simulation are presented here. Table 1 summarizes the cabin parameters for a mid-size car, represented by its wall areas, thicknesses and thermal parameters. Table 2 summarizes the operating condition parameters required to compute the cabin thermal needs. Note that the target cabin temperature is set to 23°C. The number of passengers is 0 for heating and 4 for cooling as a conservative assumption. Similarly, sun flux into the cabin is not considered when in heating mode, and it is assumed to have a direct solar irradiation ($I_{sol} = 700\ W.m^{-2}$) when in cooling mode. The vehicle speed is set to 45 km/h and the initial condition is a cabin temperature at T_{air}^{ext}.

Table 1. Vehicle cabin parameters.

Parameter	*Value*
Glazing areas	2 m^2
Opaque areas	9.9 m^2
Lateral insulation thickness	75 mm
Floor insulation thickness	15 mm
Roof insulation thickness	13 mm
Internal thermal capacity	75 $kJ.K^{-1}$
Total wall thermal capacity	155.4 $kJ.K^{-1}$
Glazing transmissivity	0.85
Wall outer absorptivity	0.85

Table 2. Operating conditions.

External temperature	Relative humidity	Convergence time	Air mass flow rate in steady state	Air mass flow rate in transient state	Recirculation ratio
T_{air}^{ext}	φ	t_{targ}	$\dot{m}_{air}^{blown}$ *Steady*	$\dot{m}_{air}^{blown}$ *Transient*	τ_{recir}
(°C)	(%)	(min)	(kg.h^{-1})	(kg.h^{-1})	(%)
-20	85	20	245	400	0
-15			236	390	
-10	95		225	360	
-5			210	330	
0		15	200	310	
5			185	290	
10		10	180	285	
15			187	290	
20			195	300	
15	95	10	187	290	0
20			195	300	0
25			248	390	50
30	85		330	533	70
35	65	15	378	608	85
40	55		400	632	88
45	35	20	408	640	

2.2 Cabin Thermal Energy needs

Figure (3) illustrates the heating and cooling thermal energy needs of the cabin as a function of external ambient temperature. Two types of curves are shown, for steady state and transient state, respectively. The steady state curves illustrate the thermal power needs to maintain the cabin at the comfort temperature of 23°C. The transient state curves illustrate the thermal power needs to bring the cabin to the comfort temperature, with the convergence time being determined according to the external temperature, as shown in Figure (4). Since there are no available data on heating and cooling convergence times, Figure (4) was developed by experimental measurement at the reference temperatures (-15°C, +20°C and +45°C) and linear interpolation in between.

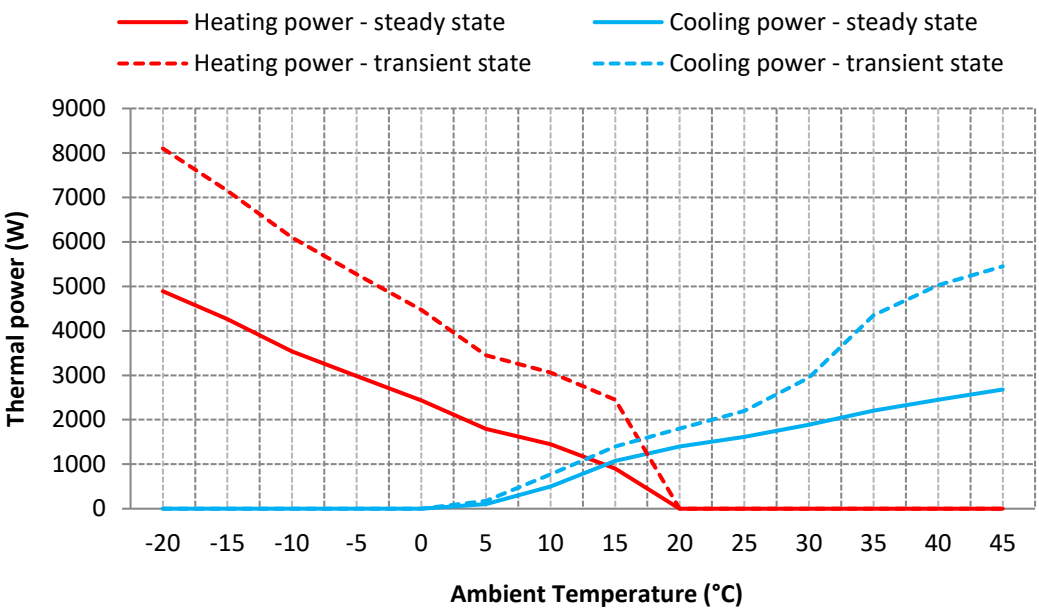

Figure (3): Thermal power function of external temperature.

Note in the above graph the presence of a zone (between 5 and 20°C) where both heating and cooling are required simultaneously. This is the zone where ambient air must be dehumidified before being heated and flowed into the cabin.

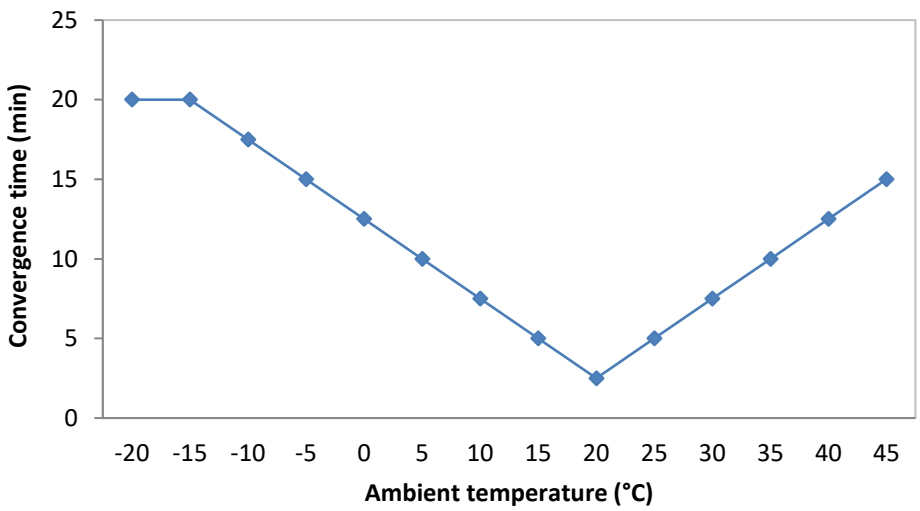

Figure (4): Convergence time as a function of the external temperature (°C).

Finally, for the range of external temperatures considered, the corresponding cabin thermal power curves are derived by combining the transient thermal power required (dashed lines in Figure 3) during the convergence time (from Figure 4) with the steady state thermal power (solid lines in Figure 3). For example, at an external temperature of -5°C, a heating power of 5,200 W is applied during the transient state over a convergence time of 15 minutes, followed by a heating power of 3,000 W during the steady state for the remaining trip duration to ensure thermal comfort of the cabin is maintained.

The range of thermal power load curves are derived by this process for all considered temperature ranges, and presented in Figure (5). This concludes the calculations under the first step of the proposed framework.

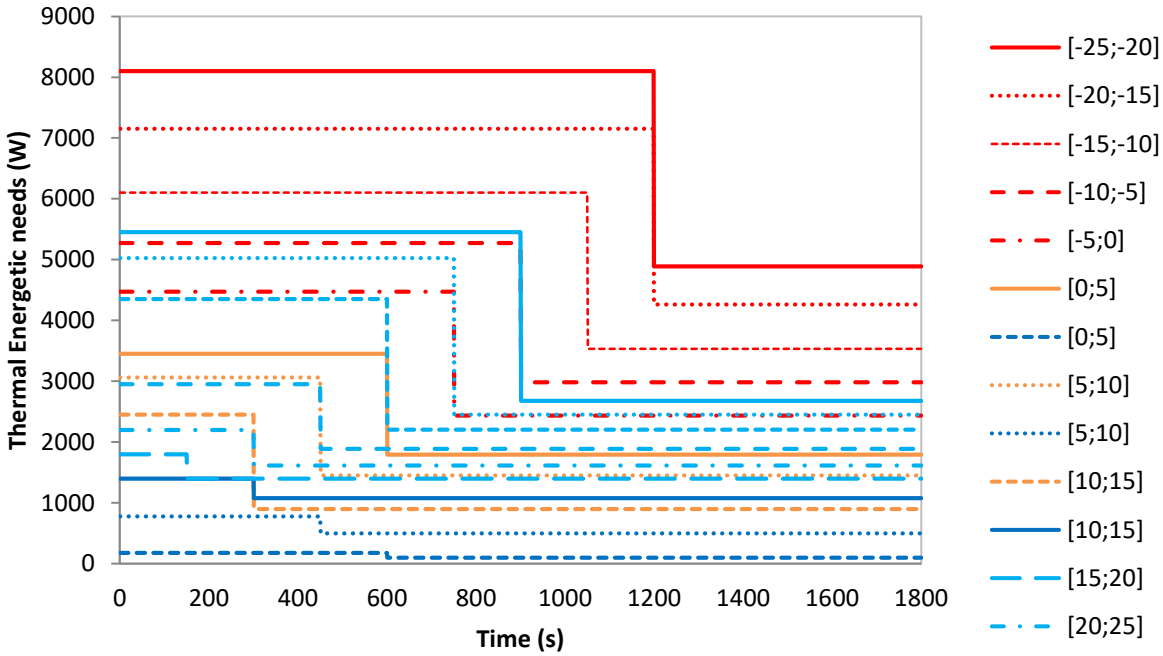

Figure (5): Heating and cooling power needs for different external temperatures.

2.3 Modified WLTP

The second step of the proposed framework, illustrated in Figure (1), involves first determining the electric consumption for powering vehicle auxiliaries. Based on a survey of industry best practice, a constant value of 750 W was assumed as an average electric consumption on middle class vehicles [20].

The second step involves weighting of the range of cabin thermal power curves obtained in step 1, using the frequency of annual temperature occurrences for a given climate. Three different climate conditions were considered corresponding to cold climate (Climate C), moderate climate (Climate M) and hot climate (Climate H), as shown in Figure (6) below.

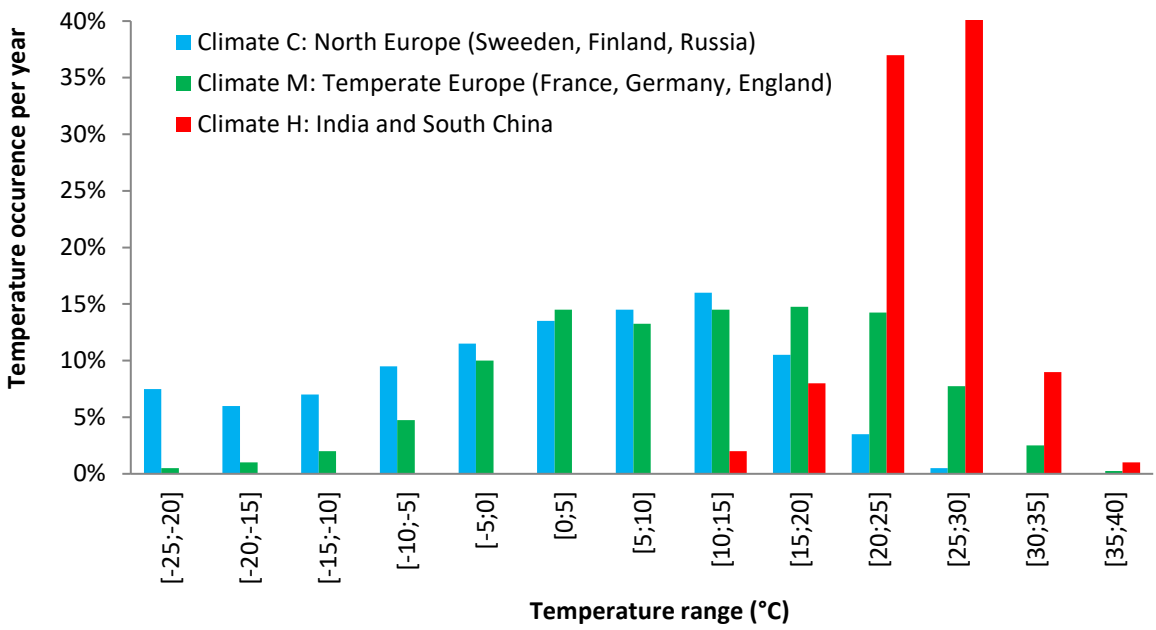

Figure (6): Percentage of temperature occurrence for the investigated cold, moderate and hot climates [21].

For each defined climate, a weighted-average cabin thermal power is computed for both heating and cooling, using equation (1):

$$P = \sum_i x_i \times P_i(T_i) \tag{1}$$

Where x_i is the percent of occurrence of annual temperature T_i, and P_i is the corresponding cabin thermal power at T_i.

The modified WLTP consists of combining the WLTC drive cycle with the heating and cooling thermal power curves and the constant electricity consumption, that now considers both mechanical power on wheels required to drive the vehicle at a given speed, and the heating and cooling thermal needs required to ensure the vehicle comfort.

The final modified WLTP is shown in Figures (7) to (9) for the three climates defined.

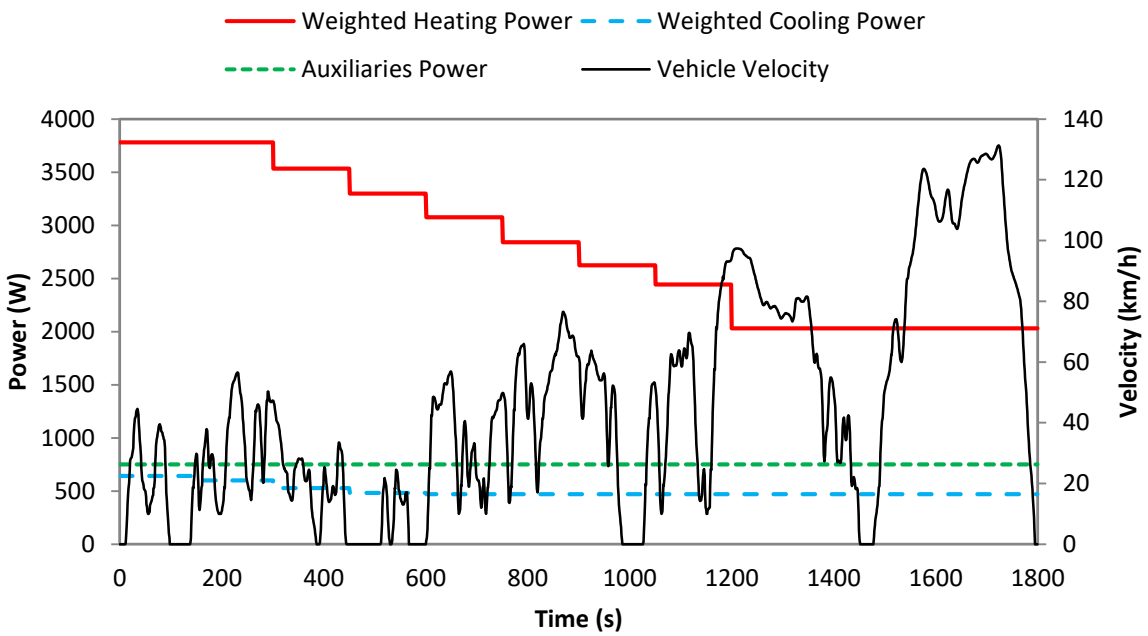

Figure (7): Modified WLTP for cold climate.

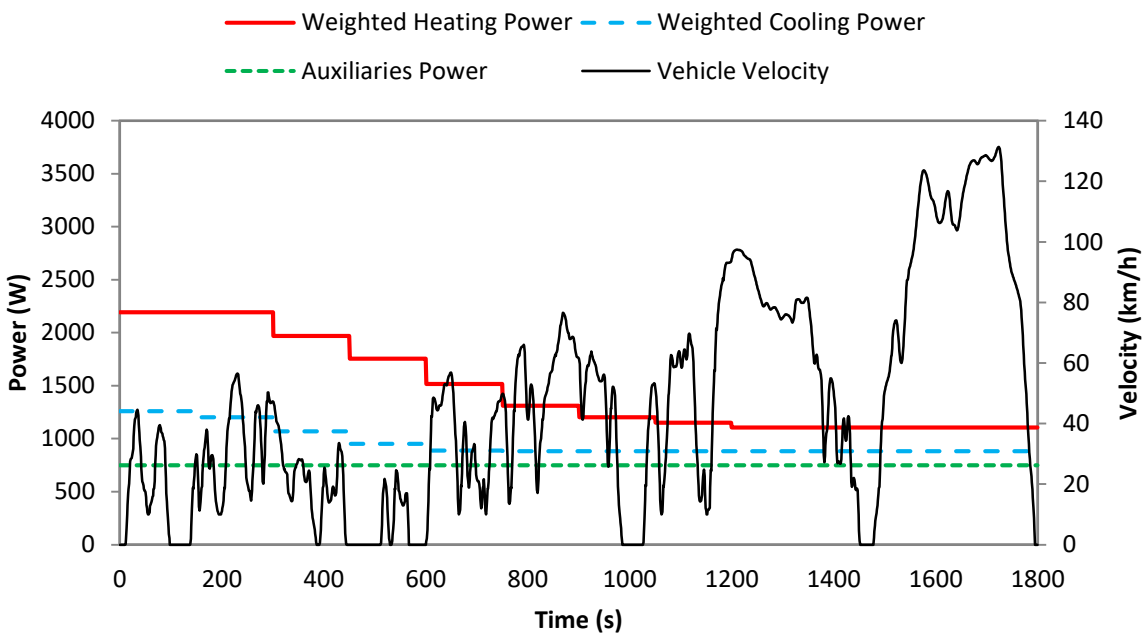

Figure (8): Modified WLTP for moderate climate.

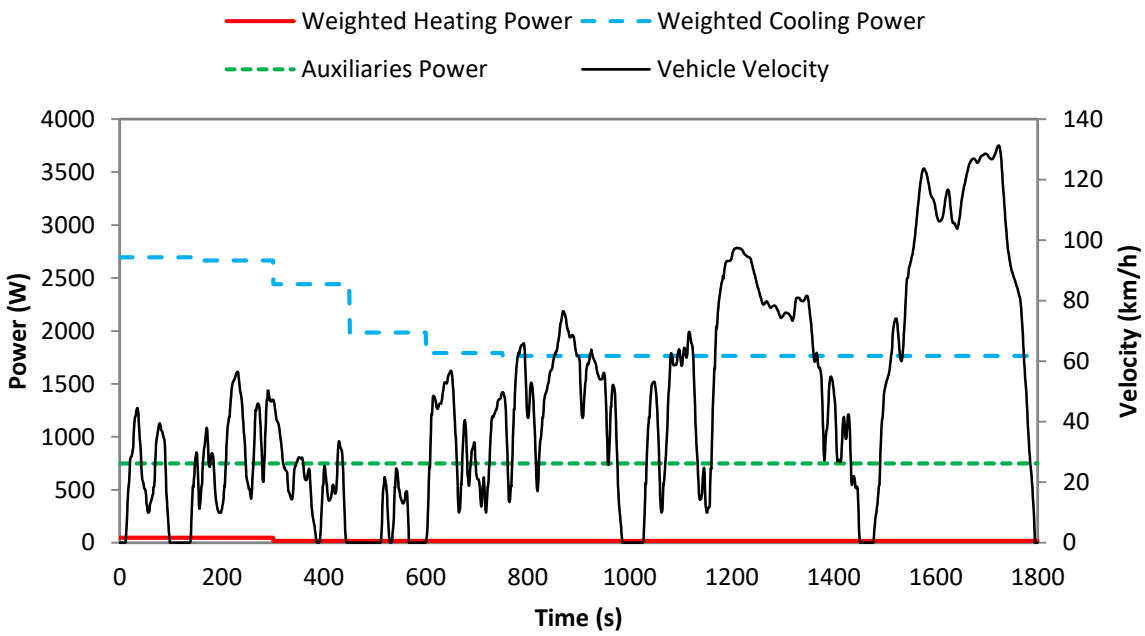

Figure (9): Modified WLTP for hot climate.

Note that the methodology adopted above to derive the modified WLTP is generalizable and can be applied for different test procedures for drive cycles, climates, and vehicle classes.

3. Vehicle model

In order to evaluate the additional fuel consumption when accounting for the thermal and electrical energy needs on top of the mechanical propulsion energy needs, a medium-class vehicle is modelled and simulated on the modified WLTP developed in Section 2.

A rechargeable hybrid electric vehicle, selected to be a series-hybrid electric vehicle (SHEV) consisting of an ICE-APU and an electric motor, was chosen for the modelling as representative of the next generation of vehicles, and due to the fact that its powertrain architecture presents additional challenges in terms of heating and cooling the cabin over conventional vehicle architectures. In conventional vehicles, the ICE assures the heating needs of the cabin through the waste engine heat, and assures the cooling needs by powering the mechanical compressor of the A/C system. In contrast, under the architecture of the modelled SHEV, the electric motor, powered by the battery, propels the vehicle, and the main purpose of the ICE is to recharge the battery when depleted, so it does not need to operate all the time. As such, other means of heating and cooling the cabin are used under this architecture. The cooling needs are assured by the battery powering an electric compressor for the A/C system with a motor efficiency ($\eta_{m,c}$) of 90% and an average coefficient of performance (COP) of 1.5 [22]. The heating needs are assured in one of two ways: by waste engine heat as in conventional vehicles when the ICE is on, or by an electric resistance powered by the battery when the ICE is off.

The series-hybrid architecture of the modelled vehicle is illustrated in Figure 10, and the development of the powertrain model is presented subsequently.

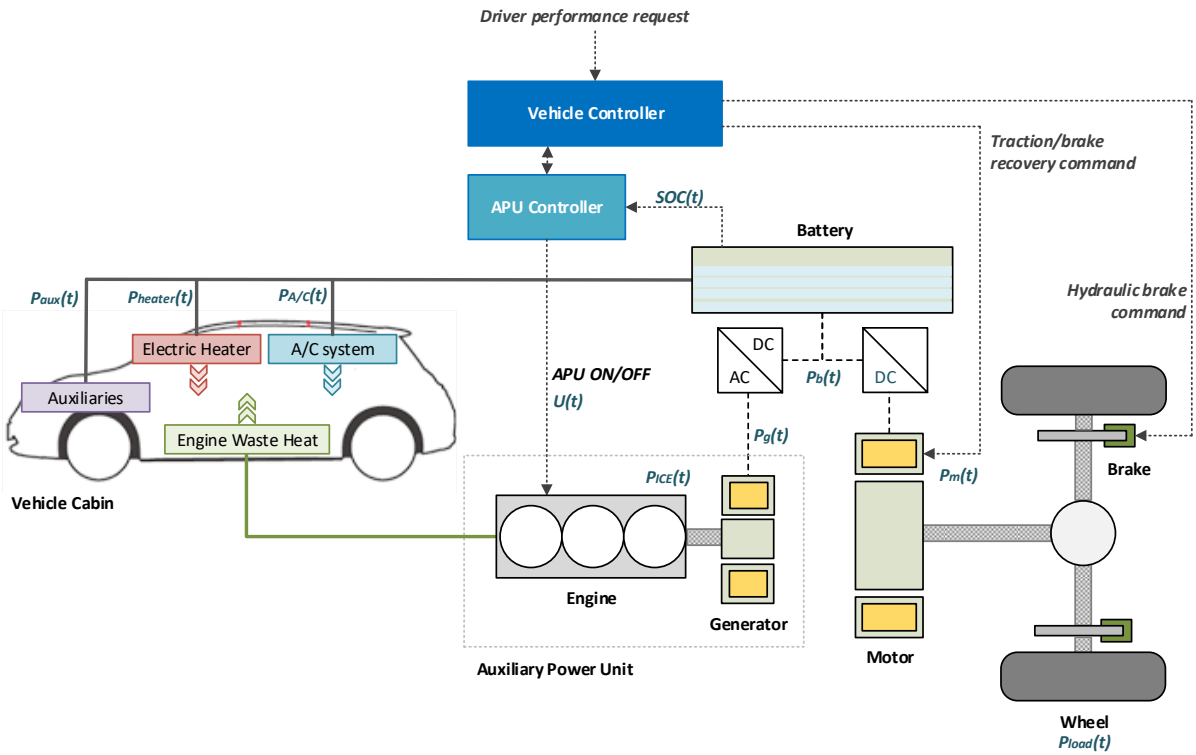

Figure 10: Series-hybrid architecture model.

The powertrain is sized in order to ensure similar performance to a medium class hybrid vehicle, with maximum velocity of 160 km/h and acceleration from 0-100 km/h in 9.6 seconds. A maximum of 80 kW tractive power is needed to accelerate the vehicle, compared to 40 kW to maintain it at 160 km/h. Consequently, the selected electric traction motor is sized at 80 kW. The APU is sized to ensure the battery sustainability under all driving conditions. [23] provides details on component sizing calculations.

As for sizing the battery, its power and capacity have to be considered. For all driving conditions, the battery must provide sufficient traction power, with the support of the APU under extreme power demand. Consequently, battery maximum power is sized with respect to the electric motor maximum power and the APU power. As a result, a battery with a power of 50 kW and a capacity of 10 kWh is considered in the analysis. The additional battery mass with the increased capacity is taken into account.

Table 2 summarizes the corresponding vehicle parameters needed for modelling the SHEV.

Table 2: Vehicle and components specifications.

Vehicle specifications	Symbol	Unit	Value
Frontal area	S	m²	2.17
Air density	ρ	kg/m3	1.205
Drag coefficient	C_D	-	0.29
Wheel friction coefficient	f_r	-	0.0106
Wheel radius	R_w	m	0.307
ICE maximum power	$P_{ICE,max}$	kW	97
ICE maximum efficiency	$\eta_{ICE,max}$	%	37
Generator maximum power	$P_{g,max}$	kW	80
Generator maximum efficiency	$\eta_{g,max}$	%	95
Traction motor maximum power	$P_{m,max}$	kW	80

Traction motor maximum efficiency[1]	$\eta_{m,max}$	%	93
Transmission ratio	i	-	5.4
Transmission efficiency	η_t	%	97
Battery maximum power	$P_{b\ max}$	kW	50
Battery capacity	C_b	kWh	10
Battery mass	M_b	kg	259
Battery state of charge	SOC	-	[0.2, 0.4, 0.6, 0.8, 1]
Battery open circuit voltage	V_{oc}	V	[220, 224, 227, 228, 251]
Battery internal resistance	R_i	Ohm	[0.315, 0.31, 0.31, 0.335, 0.385]
Vehicle mass (including driver)	M_v	kg	1210
Vehicle total mass	M_t	kg	$M_v + M_b$
Fuel heating value	H_v	MJ/kg	44.8
Auxiliaries consumption	P_{aux}	W	750
[1] The model includes a torque-speed efficiency map of the electric motor.			

Equations (3) to (10) present the powertrain model. The model calculates the power needs for traction, electric consumption and cabin thermal comfort in order to derive the final energy consumption of the vehicle. All quantities are defined in Table 2 above.

Equations (3) provides the required vehicle traction power as a function of aerodynamic parameters, rolling resisting force, inertial force, and vehicle velocity:

$$P_{load}(t) = \left(\frac{1}{2}\rho S C_D v(t)^2 + M_t g f_r\big(v(t)\big) + M_t \frac{dv(t)}{dt}\right) \times v(t) \tag{3}$$

Equation (4) provides the traction and braking power of the electric motor using the efficiencies of the motor and the transmission:

$$P_m(t) = \begin{cases} \dfrac{P_{load}(t)}{\eta_t \times \eta_m}, & \dfrac{dv}{dt} \geq 0 \\ P_{load}(t) \times \eta_t \times \eta_m, & \dfrac{dv}{dt} < 0 \end{cases} \tag{4}$$

Equation (5) calculates the power provided by the APU when the ICE is on, where $u(t)$ is the APU on/off control variable (0 for off, 1 for on):

$$P_g(t) = u(t) \times P_{ICE} \times \eta_g \tag{5}$$

Equations (6) provides the battery power consumption which depends on the power of the electric motor power, the auxiliaries, the electric heater and the air-conditioning, supplemented by the APU power when on.

$$P_b(t) = P_m(t) + P_{aux}(t) + P_{heater}(t) + P_{A/C}(t) - P_g(t) \tag{6}$$

Where $P_{A/C}(t)$ is given by Equation (7):

$$P_{A/C}(t) = \frac{P_{cooling}(t)}{\eta_{m,c} \times COP} \tag{7}$$

Note that the auxiliaries draw constant power, and the cooling and heating power are as derived in Section 2.

Therefore, the electric consumption can now be calculated by Equation (8):

$$I_b(t) = \frac{V_{oc}\big(SOC(t)\big) - \sqrt{V_{oc}^2\big(SOC(t)\big) - 4P_b(t)R_i\big(SOC(t)\big)}}{2R_i\big(SOC(t)\big)} \tag{8}$$

Where SOC is given by Equation (9):

$$SOC(t) = SOC_i(t) + \frac{1}{C_b}\int_{t_0}^{t} I_b(t)dt \tag{9}$$

Finally, the vehicle fuel consumption is found by Equation (10):

$$\dot{m}_f(t) = \begin{cases} \dfrac{P_{ICE}(t)}{\eta_{ICE} \times H_v}, & APU{:}ON \\ 0, & APU{:}OFF \end{cases} \tag{10}$$

Two distinct controllers are considered in the model as illustrated in Figure 10: the vehicle controller and the APU controller. The vehicle controller is in charge of meeting the driver request in terms of performance. Hence, its main objective is to control the electric motor power in order to meet the traction and brake energy recovery demand, as presented in equation (4). The APU controller monitors the battery SOC; thus, it controls the APU operations in order to maintain the SOC in the desired range. Therefore, an engine on/off variable $u(t)$ is considered in equation (5) in order to control the APU start operations. $u(t)$ takes the value of 0 for APU-off and 1 for APU-on.

Dynamic programming (DP) is used in this study in order to provide the global optimal strategy to control the APU operations [24]. The choice of dynamic programming over traditional rule-based energy management strategies is to ensure that only the impact of the cabin thermal and auxiliary needs are assessed, thereby excluding the potential bias of rule-based strategies on fuel consumption [25]. It decides on the optimal strategy $U_{opt} = \{u(1), \dots, u(N)\}_{opt}$ for the scheduled route at each instant t while minimizing the fuel cost function J presented in equation (11). Consequently, DP computes backward in time from the final desired battery state of charge SOC_f to the initial state SOC_i the optimal fuel mass flow rate $\dot{m}_f\big(SOC(t), u(t)\big)$ in the discretized state time space as per equations (12) to (14). The generic DP function presented in [26] is considered in this study, with the battery SOC as state variable $x(t)$ and the APU on/off as control variable $u(t)$.

During APU operations, the ICE is allowed to operate at any point of its torque-speed map; however, the energy management strategy tends to maximize the powertrain efficiency by operating the engine on its optimal operating line.

Note that the resulting optimal APU on/off strategy U_{opt} must not cause the components to violate their relevant physical boundary constraints in terms of speed, power or SOC, in order to ensure their proper functioning within the normal operation range. These constraints are included in the DP model and summarized in equations (15) to (22). It is also noteworthy to mention that using DP as APU energy management strategy excludes the impact of rule-based energy management strategies currently used on hybrid vehicles on the consumption. Consequently, the obtained fuel consumption results with DP are only dependant on the investigated powertrain components and their respective efficiencies.

$$J = min\left\{\sum_{t=1}^{N} \dot{m}_f\big(SOC(t), u(t)\big) \times dt_s\right\} \tag{11}$$

with

discrete step time: $$dt_s = 1 \tag{12}$$

number of time instances: $N = \frac{n}{dt_s}$ (with n the time length of the driving cycle) (13)

state variable equation: $$SOC(t+1) = f\big(SOC(t), u(t)\big) + SOC(1) \tag{14}$$

initial SOC: $$SOC(1) = SOC_i \tag{15}$$

final SOC: $$SOC(N) = SOC_f \tag{16}$$

SOC constraint: $$SOC(t) \in [0.2, 0.9] \tag{17}$$

battery power constraint: $$P_{b_{min}} \leq P_b(t) \leq P_{b_{max}} \tag{18}$$

motor torque constraint: $$P_{m_{min}}\big(\omega_m(t)\big) \leq P_m(t) \leq P_{m_{max}}\big(\omega_m(t)\big) \tag{19}$$

motor speed constraint $$0 \leq \omega_m(t) \leq \omega_{m_{max}}(t) \tag{20}$$

generator power constraint: $$P_{g_{min}}\big(\omega_m(t)\big) \leq P_g(t) \leq P_{g_{max}}\big(\omega_m(t)\big) \tag{21}$$

generator speed constraint: $$0 \leq \omega_g(t) \leq \omega_{g_{max}}(t) \tag{22}$$

4. Results and discussion

The potential of fuel savings of ICE-APU was simulated over a sequence of three-repeated WLTC driving cycles (23 km each) covering driving distances up to around 69 km. Simulations are performed at an initial SOC of 80% and a final SOC by the end of the trip at 30%.

Simulations are performed on a baseline scenario similar to current fuel consumption on standard regulatory drive cycles where only propulsion energy needs are accounted, and four additional scenarios accounting for different cooling, heating and electric consumption needs. In all scenarios considered, the electric auxiliaries draw constant energy from the battery, and the cooling needs are ensured by the A/C system driven by the electric compressor using energy from the battery. The heating needs are normally ensured by engine waste heat when the engine is on. When the engine is off, other means are needed to heat the cabin. In the

considered scenarios, two options are included: storing excess engine waste heat when the engine is on, to be used later for heating the cabin when the engine is off; or, an electric heater where electricity from the battery powers a resistance to heat the air.

- Baseline: Only mechanical propulsion needs on a sequence of 3 WLTC drive cycles
- Scenario 1: Baseline + continuous electric auxiliaries needs of 750W
- Scenario 2: Scenario 1 + cabin cooling ensured by A/C + heating ensured by stored engine waste heat
- Scenario 3: Scenario 1 + cabin cooling ensured by A/C + cabin heating ensured by electric heater when engine is off, or by engine waste heat when engine is on
- Scenario 4: Scenario 1 + cabin cooling ensured by A/C + cabin heating needs always ensured by electric heater

Figure (11) shows the fuel consumption as a function of the different considered scenarios for different climates.

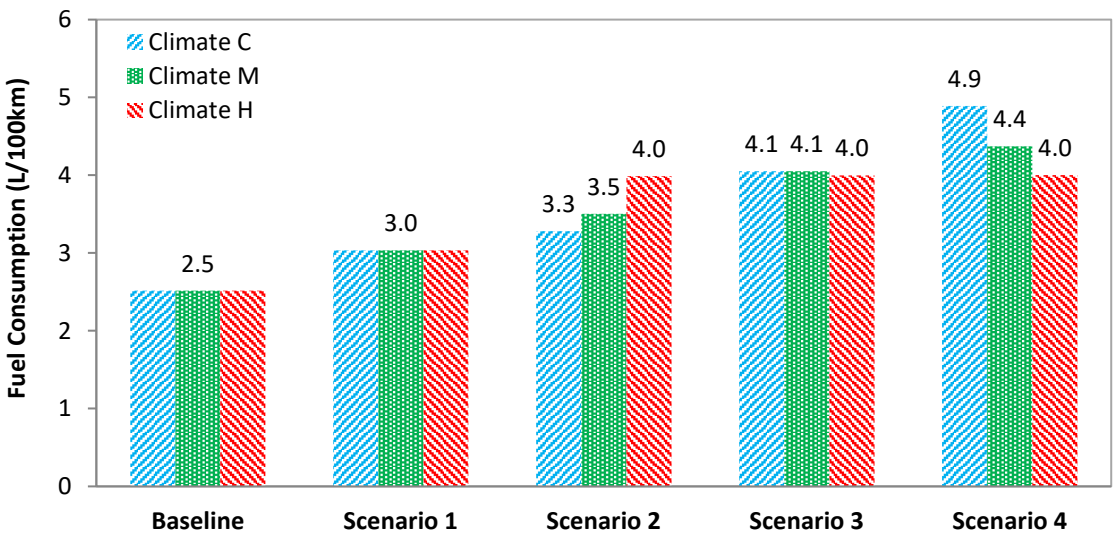

Figure (11): Fuel consumption simulation results of the modelled rechargeable hybrid vehicle under the three investigated climates.

Several conclusions can be drawn from the simulation results. First, it is clear that the fuel consumption under each of the four scenarios, which consider cabin thermal and vehicle electric needs, is notably higher than the baseline for all climates considered. This means that despite the introduction of the new WLTP, the current industry estimates for fuel consumption still under estimate the real-world driving consumption.

In scenario 1, the vehicle electric needs increase the fuel consumption by around 20% regardless of climate condition since the electric consumption is assumed to be constant. This shows that the electric consumption of auxiliaries should not be neglected, and it would be beneficial to explore ways to reduce this consumption on-board.

In scenario 2, the cabin cooling needs provided by the AC system have considerable negative effect on fuel consumption especially in hot climates, increasing by about 1.5 L/100km, or on

average by 43% over the baseline. Therefore, the cooling needs need to be accounted for in consumption assessments.

In scenario 3, the cabin heating needs increase the fuel consumption by about 1.5 L/100km for all climates, which is a notable 59% over the baseline, and that despite the use of waste heat recovery from the engine when operating. This shows that, similar to cooling, the heating needs also need to be considered in consumption assessments.

In scenario 4, the cabin heating needs significantly affect the fuel consumption, especially in cold climates, by about 96% over the baseline, almost equal to the fuel consumption needed for traction. This is due to the reliance on the battery to power the heater, which requires the engine to operate longer in order to charge the battery, without any recovery of its waste heat. This highlights, from an energy standpoint, the performance challenges currently faced by electric vehicles in cold climates in terms of range and consumption.

From the analysis above, it can be concluded that in order to more accurately estimate powertrain efficiency of rechargeable electric vehicles, the additional energy consumption for cooling, heating and electric needs should be considered. To that end, the overall powertrain efficiency equation is expanded to include the thermal comfort energy requirements, in addition to the mechanical traction needs normally considered. Thus, the overall powertrain efficiency is calculated as the ratio of the total energy demand for traction, thermal comfort and auxiliaries over the total energy supply which includes the fuel energy, the brake recovery energy, and the electric energy from the grid for charging the battery, as shown in Equation (23).

$$\eta_{powertrain} = \frac{E_{traction} + E_{auxiliaires} + E_{cooling} + E_{heating}}{E_{ber} + E_{fuel} + E_{grid}} \tag{23}$$

Using the equation above, Figure (12) shows the overall powertrain efficiency trends for the baseline and the four scenarios considered under the cold, moderate and hot climates.

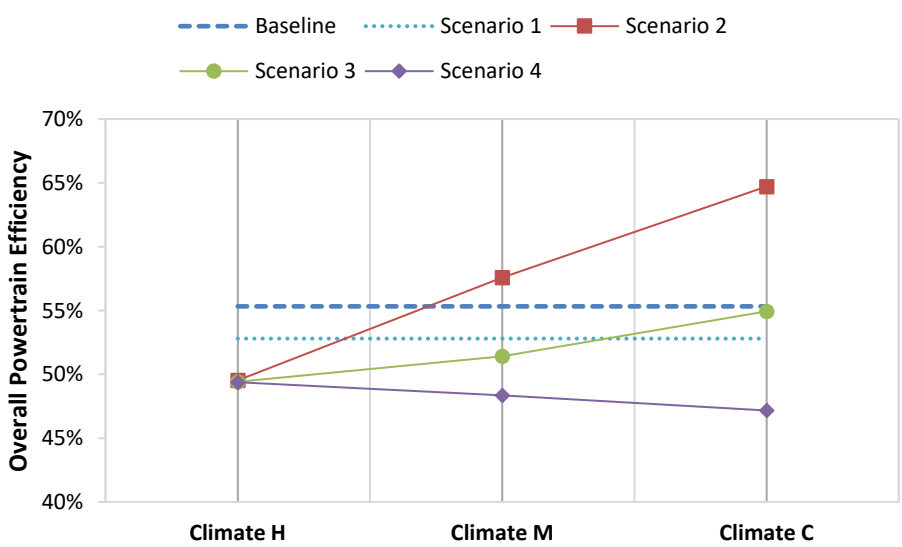

Figure (12): Overall powertrain efficiency for the three investigated climates under the baseline and the three cabin heating scenarios.

The baseline represents the powertrain efficiency as typically calculated in terms of traction energy consumption per total energy consumed, without considering electric and thermal comfort needs.

In scenario 1, accounting for the auxiliaries' electric consumption impacts the powertrain efficiency by a constant reduction of 4.5% below the baseline, as expected.

In scenarios 2 to 4 where cooling and heating needs are considered, there are different impacts on the powertrain efficiency due to the different heating means employed. As shown in scenarios 2 and 3, the more heating needs are ensured by engine waste heat recovery, the better the overall powertrain efficiency [27, 28], especially in colder climates where heating needs are high. This means that in cold climates, having an ICE is beneficial, which favors the use of rechargeable electric vehicles in these climates.

In contrast, powertrain efficiency is lowest in scenario 4, especially under colder climates when heating needs are ensured entirely by the electric heater, which incurs additional fuel consumption. This confirms that in cold climates electric vehicle configurations without an ICE are less efficient than rechargeable electric vehicles when thermal needs are considered.

In summary, the above analysis shows that accounting for electric and thermal comfort needs not only affects the consumption on the WLTC drive cycle, but also the overall powertrain efficiency depending on the strategy used for cabin heating. It is therefore beneficial to consider alternative heating technologies in future designs, such as heat pumps and heat recovery schemes [29]

5. Conclusion

In light of recent controversy regarding the consumption gap between real world driving conditions and OEMs regulatory driving tests, there is interest in closing this gap by assessing additional sources of consumption not currently accounted for in regulatory drive tests, such as passengers' thermal comfort and auxiliary electric needs. Hence, this study presents a framework for assessing the impact of cabin cooling and heating in addition to electric auxiliary needs on vehicle consumption on the WLTP under different climate conditions.

To that end, a vehicle cabin model was developed, and a methodology was presented to generate the average heating and cooling power profiles as function of the ambient external temperature. Three climate conditions were considered (hot, moderate and cold) for that purpose. Constant electric power consumption was assumed representing the average auxiliary consumption in modern vehicles. The outcome from this approach is a modified WLTP combining the generated power profiles with the WLTC drive cycle, thereby combining the vehicle thermal comfort and auxiliary needs with the required mechanical power to drive the vehicle.

The additional energy consumption on the modified WLTP was assessed for a rechargeable series hybrid electric vehicle (SHEV). An SHEV powertrain model was developed and the dynamic programming optimal management strategy was used to control the energy distribution between the fuel tank and the battery.

Simulation results showed that the electric consumption of auxiliaries should not be neglected since an auxiliary's load of 750W causes 20% increase in fuel consumption on an SHEV. Similarly, cabin thermal comfort needs significantly affect the fuel consumption (up to 43% increase due to cabin cooling, and up to 59% due to cabin heating).

Furthermore, when heating is done solely by electric heaters without heat recovery from the engine, the additional consumption almost equals the fuel consumption needed for traction. Therefore, relying on waste heat recovery from the engine to heat the cabin in cold climates can be very beneficial for improving the overall powertrain efficiency. A relevant conclusion for OEMs is that considering appropriate means and strategies for cabin heating and cooling according to local climate conditions can maximize vehicle efficiency for different regions of the world. For instance, OEMs could provide different cabin comfort technologies for a certain vehicle model according to the climate conditions of the considered market. Therefore future research could build on this work by exploring different component technologies (such as the use of heat pumps for both heating and cooling needs) and their impact on fuel consumption.

In conclusion, it is necessary to account for cabin thermal comfort and auxiliary needs in vehicle consumption estimation under regulatory drive tests, which will allow for closing the gap with real world driving performance.

6. References

[1] A. MAROTTA, J. PAVLOVIC, B. CIUFFO, S. SERRA, G. FONTARAS, "Gaseous Emissions from Light-Duty Vehicles - Moving from NEDC to the New WLTP Test Procedure", European Comission-Joint Research Center, Institute for Energy and Transport, Sustainable Transport Unit, Ispra 21027, Italy. Environmental Science & Technology.

[2] D. Tsokolis, S. Tsiakmakis, A. Dimaratos, G. Fontaras, P. Pistikopoulos, B. Ciuffo, Z. Samaras, Fuel consumption and CO2 emissions of passenger cars over the New Worldwide Harmonized Test Protocol, Applied Energy, Volume 179, October 2016, Pages 1152-1165

[3] P. MOCK, J. KÜHLWEIN, U. TIETGE, V. FRANCO, A. BANDIVADEKAR, J. GERMAN, "The WLTP - How a new test procedure for cars will affect fuel consumption values in the EU", The International Council On Clean Transportation, October 2014

[4] L. SILEGHEM, D. BOSTEELS, J. MAY, C. FAVRE, S. VERHELST, "Analysis of Vehicle emission measurements on the new WLTC, the NEDC and the CADC", Elsevier, Transportation Research Part D: Transport and Environment, Volume 32, October 2014, Pages 70-85

[5] J. DEMUYNCK, D. BOSTEELS, M. DE PAEPE, C. FAVRE, J. MAY, S. VERHELST, « Recommendations for the new WLTP cycle based on an analysis of vehicle emission measurements on NEDC and CADC », Elsevier, Energy Policy, Volume 49, October 2012, Pages 234-242.

[6] D. Tsokolis, A. Dimaratos, Z. Samaras, S. Tsiakmakis, G. Fontaras and Biagio Ciuffo, "Quantification of the effect of WLTP introduction on passenger cars CO2 emissions", Journal of Earth Sciences and Geotechnical Engineering, vol.7, no. 1, 2017, 191-214

[7] R. Farrington, R. Anderson, D. Blake, S. Burch, M. Cuddy, M. Keyser and J. Rugh, Challenges and Potential Solutions for Reducing Climate Control Loads in Conventional and Hybrid Electric Vehicles. VTMS4, 1999

[8] Richard 'Barney' Carlson, Matthew G. Shirk and Benjamin M. Geller, "Factors Affecting the Fuel Consumption of Plug-In Hybrid Electric Vehicles", Presented at the 25th World Battery, Hybrid and Fuel Cell Electric Vehicle Symposium & Exhibition, Shenzhen, China, 2010

[9] R. Farrington and J. Rugh, "Impact of Vehicle Air-Conditioning on Fuel Economy, Tailpipe Emissions, and Electric Vehicle Range", National Renewable Energy Laboratory (NREL), 2000

[10] R. Farrington, M. Cuddy, M. Keyser and J. Rugh, Opportunities to Reduce Air Conditioning Loads through Lower Cabin Soak Temperatures. NREL Report No. CP-540-26615, Golden, CO: National Renewable Energy Laboratory, 1999

[11] Chiara Fiori, Kyoungho Ahn and Hesham A. Rakha, Power-based electric vehicle energy consumption model: Model development and validation, Applied Energy 168(2016) 257-268

[12] Johnson, V., "Fuel Used for Vehicle Air Conditioning: A State-by-State Thermal Comfort-Based Approach," SAE Technical Paper 2002-01-1957, 2002, doi:10.4271/2002-01-1957.

[13] Kiran R. Kambly and Thomas H. Bradley, Estimating the HVAC energy consumption of plug-in electric vehicles, Journal of Power Sources, 259(2014) 117-124

[14] D. Clodic, E. Zgheib, S. Mortada, Impacts of heating and cooling on electrified vehicles, in: 4th European Workshop Mobile Air Conditioning and Vehicle Thermal Systems 2011, Torino, 2011.

[15] Ziqi Zhang, Wanyong Li, Chengquan Zhang, Jiangping Chen, Climate control loads prediction of electric vehicles, Applied Thermal Engineering, 110(2017) 1183-1188

[16] Rask, E., “Ford Focus BEV In-depth (Level 2) Testing and Analysis,” Presented at Vehicle Systems Analysis Technical Team (VSATT) meeting, Apr. 2014.

[17] Slezak, L., “EV Everywhere Grand Challenge: Auxiliary Systems Energy Requirements,” Presented at EV Everywhere workshop, Sept. 2012.

[18] Matthew A. Jeffers, Larry Chaney, and John P. Rugh, Climate Control Load Reduction Strategies for Electric Drive Vehicles in Warm Weather, National Renewable Energy Laboratory, SAE Technical Paper 2015-01-0355, 2015, doi: 10.4271/2015-01-0355

[19] Breque, F., 2017. Cabin Thermal Needs : Modeling and Assumption Analysis, in: International Modelica Conference. Prague, Czech Republic.

[20] Johannes Liebl, Stephan Neugebauer, Andreas Eder, Matthhias Linde, Boris Mazar, Wolfgang Stütz, “The Thermoelectric Generator from BMW is Making Use of Waste Heat”, MTZ 01/2009, Volume 70

[21] Weather data. Retrieved from National Renewable Energy Laboratory: https://sam.nrel.gov/weather

[22] Shu Jun Wang, Jun Jie Gu, “Experimental Analysis of an Automotive Air Conditioning System With Two-Phase Flow Measurements”, International Refrigeration and Air Conditioning Conference, 2004

[23] W. Bou Nader, C. Mansour, O. Guezet and M. Nemer, « exergo-technological explicit methodology for gas-turbine system optimization for series hybrid electric vehicles », Journal of Automobile Engineering, Part D, JAUTO-17-0072

[24] Mansour C and Clodic D. Optimized energy management control for the Toyota Hybrid System using dynamic programming on a predicted route with short computation time. Int J Automot Technol 2012; 13: 309–324.

[25] Mansour C. Trip-based optimization methodology for a rule-based energy management strategy using a global optimization routine: the case of the Prius plug-in hybrid electric vehicle. In: Proceedings of the Institution of Mechanical Engineers. Part D: Journal of Automobile Engineering, Vol 230, Issue 11, pp. 1529 – 1545, 2015.

[26] Sundstrom O and Guzzella L. A generic dynamic programming Matlab function. *2009 IEEE Control Applications, (CCA) & Intelligent Control, (ISIC)*. St. Petersburg, 2009, pp. 1625-1630. doi: 10.1109/CCA.2009.5281131

[27] Dimitrova, Z., & Maréchal, F. (2015). Energy integration on multi-periods and multi-usages for hybrid electric and thermal powertrains. Energy, 83, 539-550.

[28] Dimitrova, Z., & Maréchal, F. (2015). Energy integration study on a hybrid electric vehicle energy system, using process integration techniques. Applied Thermal Engineering, 91, 834-847.

[29] Dimitrova, Z., & Maréchal, F. (2017). Energy integration on multi-periods for vehicle thermal powertrains. The Canadian Journal of Chemical Engineering, 95(2), 253-264.